Supporting Information

Biomimetic Aligned Micro-/Nanofibrous Composite Membranes with Ultrafast Water Transport and Evaporation for Efficient Indoor Humidification

Jingxiu Chen,[†] Jianzhang Mai,[‡] Chao Wang,[†] Yanyan Lin,[†] Dongyang Miao,[†] Yongqiang Lin,[§] Aijaz Ahmed Babar,[†,∥] Xianfeng Wang,*[,†,⊥] Jianyong Yu*[,†] and Bin Ding[†]

[†]Innovation Center for Textile Science and Technology, College of Textiles, Donghua University, Shanghai 201620, China

[‡]Guangdong Midea Refrigeration Equipment Co., Ltd., Foshan, Guangdong 528311, China

[§]Qing Yuan Polytechnic, Qingyuan, Guangdong 511510, China

[∥]Textile Engineering Department, Mehran University or Engineering and Technology, Jamshoro 76060, Pakistan

[⊥]College of Textiles Science and Engineering, Wuhan Textile University, Wuhan 430073, China

*Email: wxf@dhu.edu.cn.

*Email: yujy@dhu.edu.cn.

Supplementary Information contains:

Supplementary Figures S1-S13

Supplementary Tables S1-S3

Supplementary Movies S1-S7

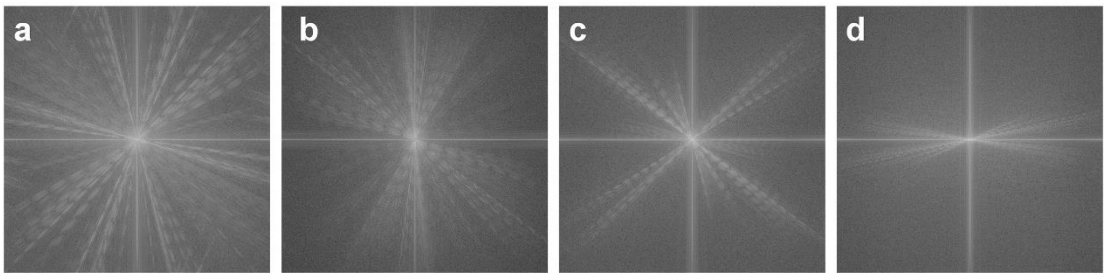

Figure S1. 2D-FFT for PAN NFMs at various RH of (a) 25%, (b) 45%, (c) 65%, and (d) 85%.

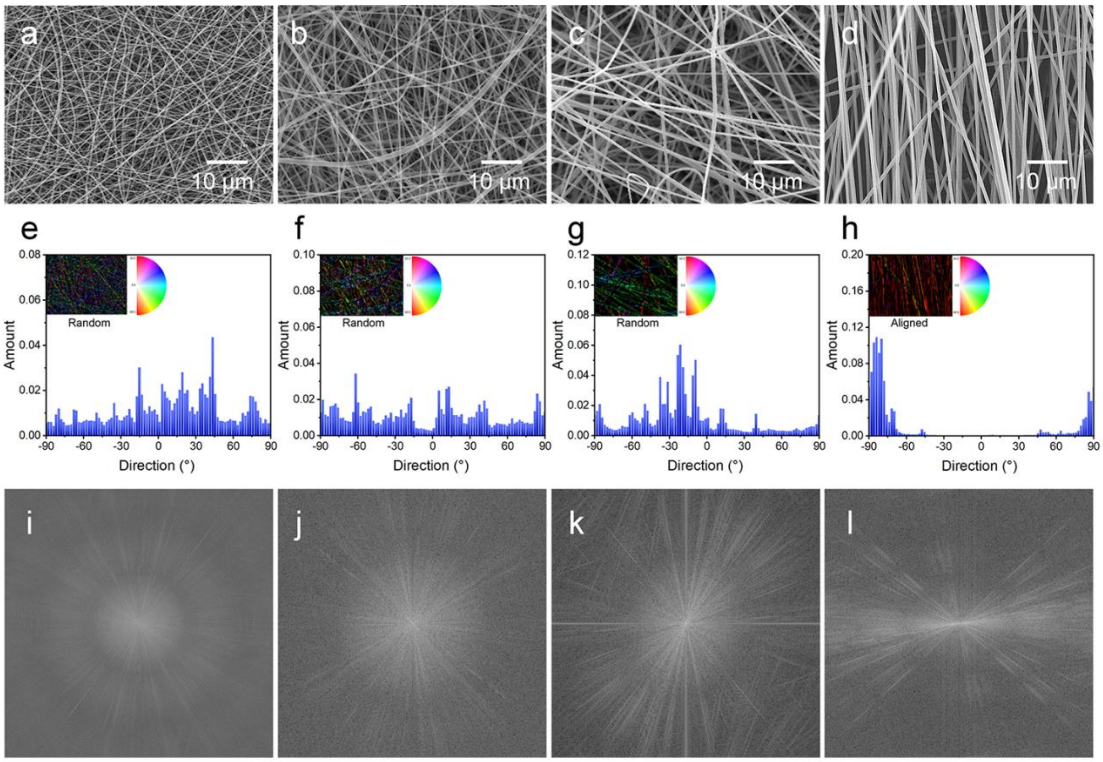

Figure S2. SEM images of PAN NFMs at various RH of (a) 25%, (b) 45%, (c) 65%, and (d) 85%. (e–h) Directionality histograms for PAN NFMs in (a–d). Color images of nanofibers indicate the angle mapping of fiber orientations. (i–l) 2D-FFT for PAN NFMs in (a–d).

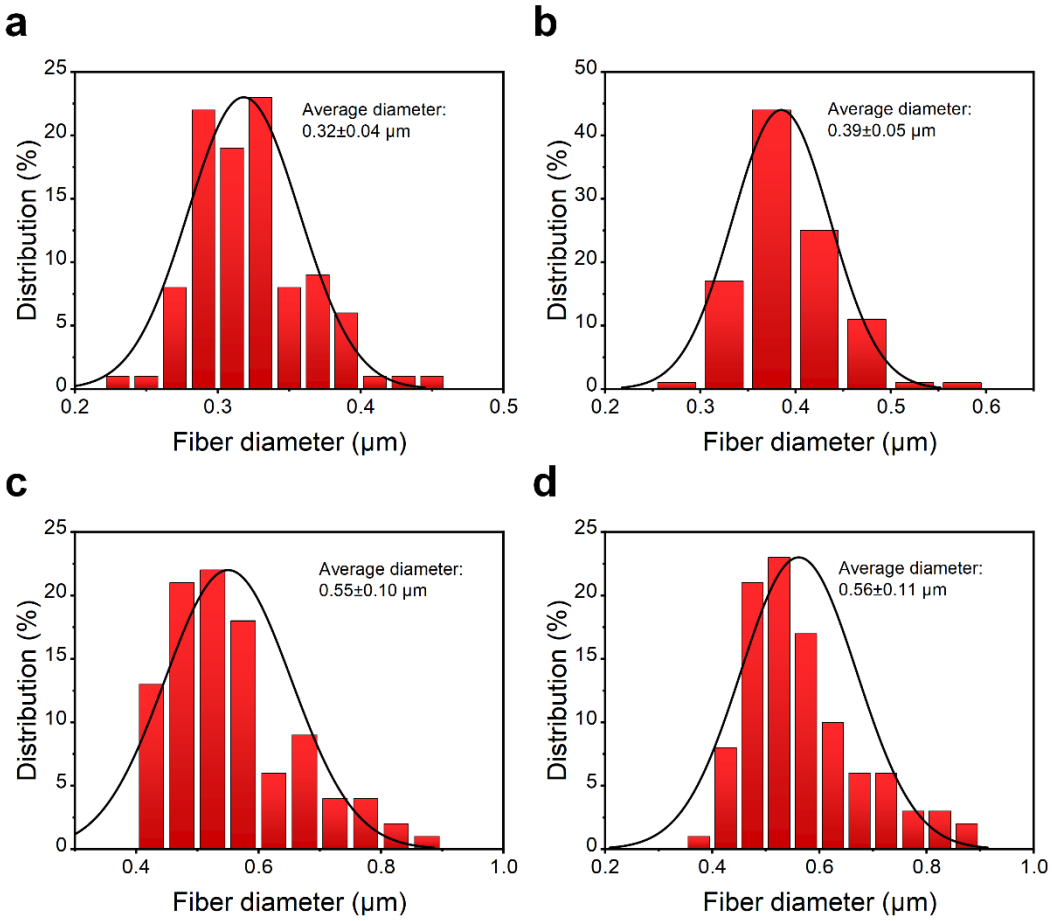

Figure S3. Fiber diameter distribution of PAN NFMs at different RH of (a) 25%, (b) 45%, (c) 65%, and (d) 85%.

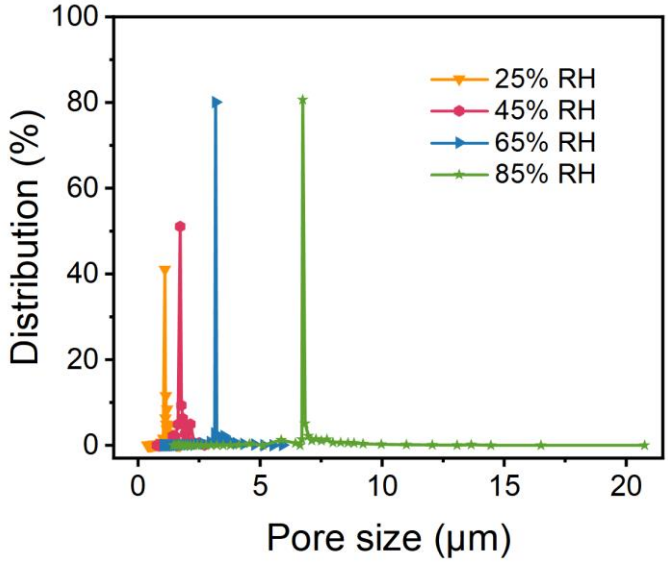

Figure S4. Pore size distribution of PAN NFMs at different RH of (a) 25%, (b) 45%, (c) 65%, and (d) 85%.

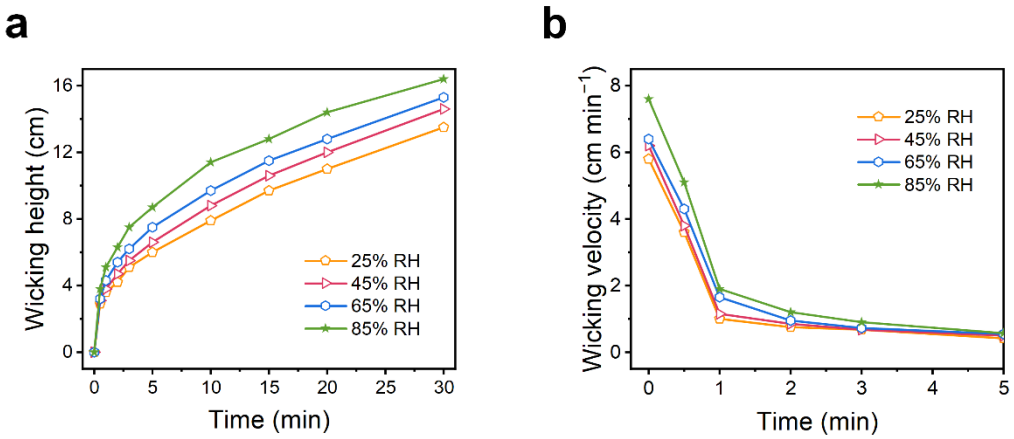

Figure S5. Wetting behavior of the micro-/nanofibrous composite membranes at different RH: (a) wicking height and (b) wicking velocity.

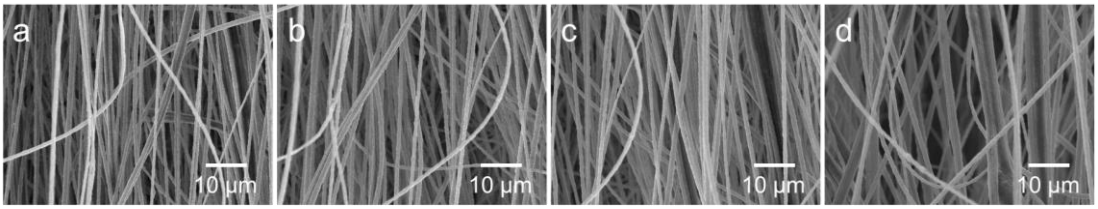

Figure S6. SEM images of PAN-SiO_2 NFMs with various concentrations of SiO_2 NPs: (a) 5 wt %, (b) 10 wt %, (c) 20 wt %, and (d) 30 wt %.

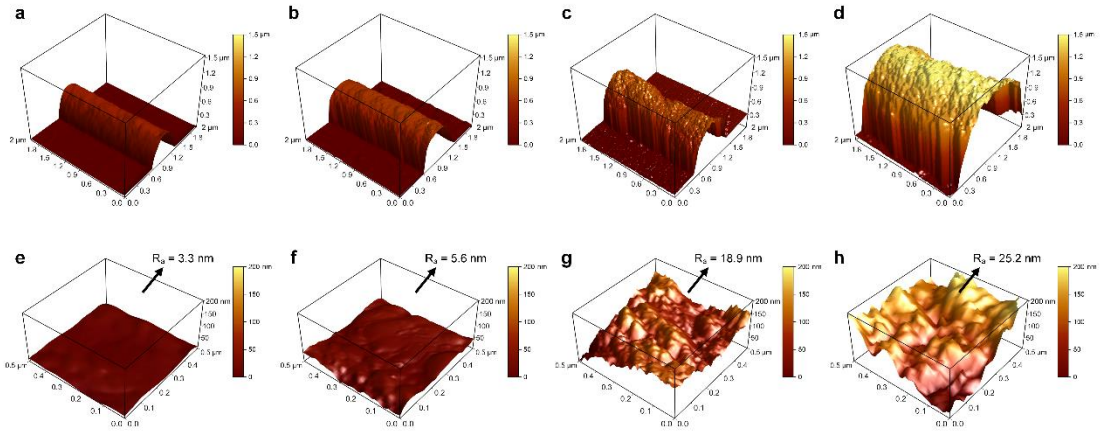

Figure S7. (a-d) 3D AFM images of the original PAN-SiO_2 nanofibers with various concentrations of SiO_2 NPs: (a) 0 wt %, (b) 5 wt %, (c) 10 wt %, and (d) 30 wt %. The images were further plane fitted to calculate the average roughness of the corresponding (e) PAN-SiO_2-0, (f) PAN-SiO_2-5, (g) PAN-SiO_2-10, and (h) PAN-SiO_2-30 fiber.

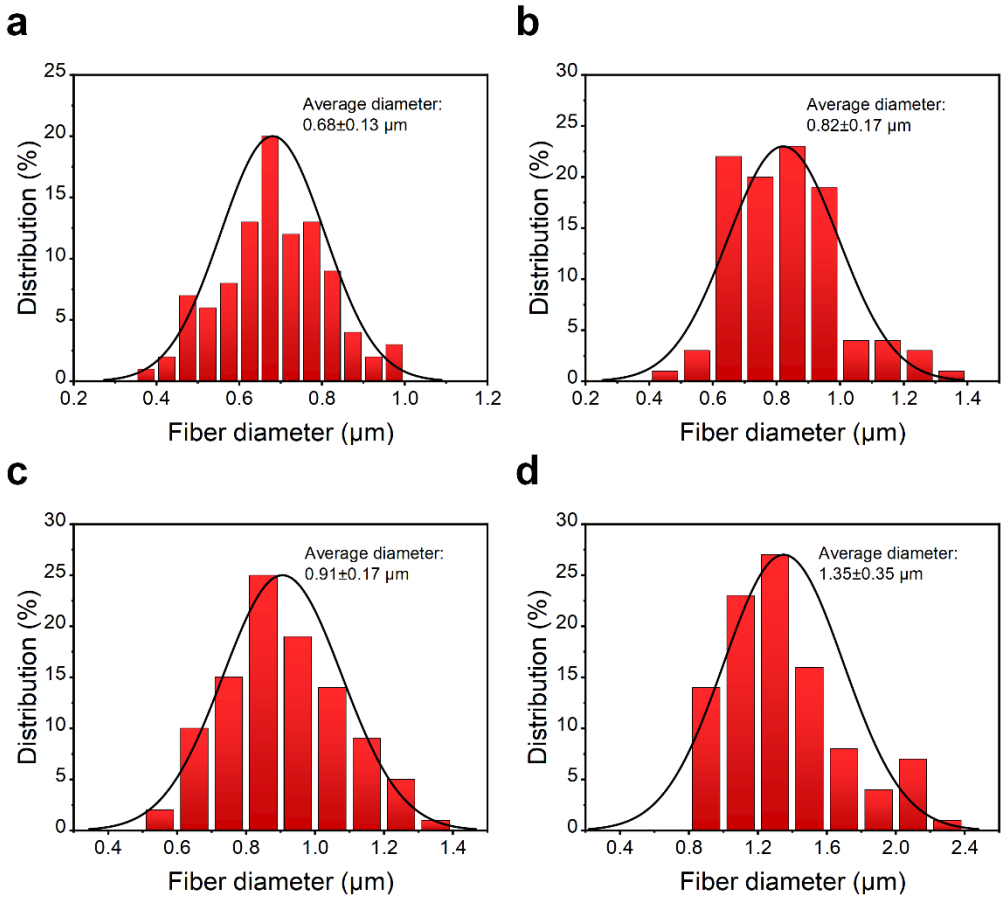

Figure S8. Fiber diameter distribution of PAN-SiO_2 NFMs with various concentrations of SiO_2 NPs: (a) 5 wt %, (b) 10 wt %, (c) 20 wt %, and (d) 30 wt %.

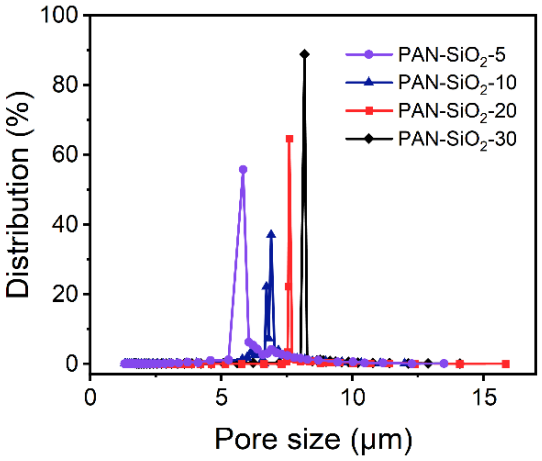

Figure S9. Pore size distribution of PAN-SiO_2 NFMs with various concentrations of SiO_2 NPs: (a) 5 wt %, (b) 10 wt %, (c) 20 wt %, and (d) 30 wt %.

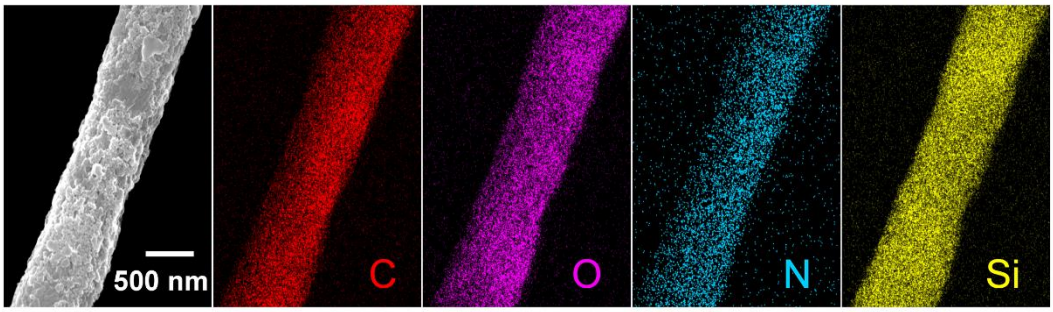

Figure S10. FE-SEM image and corresponding elemental maps of PAN-SiO_2-20 nanofiber.

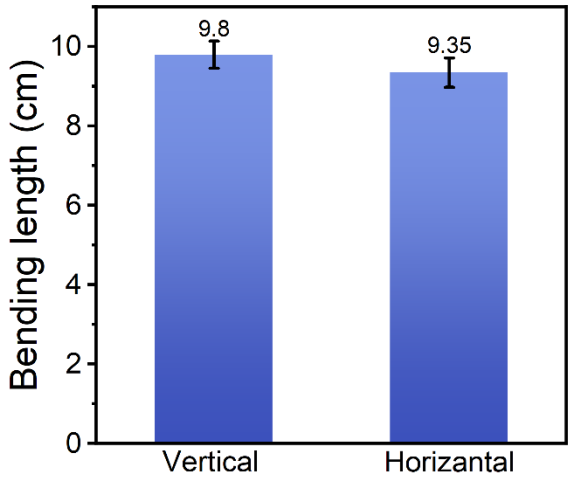

Figure S11. The mechanical stiffness of PAN nanofiber/NW composite membrane. The vertical and horizontal bending lengths were 9.8 cm and 9.35 cm, respectively.

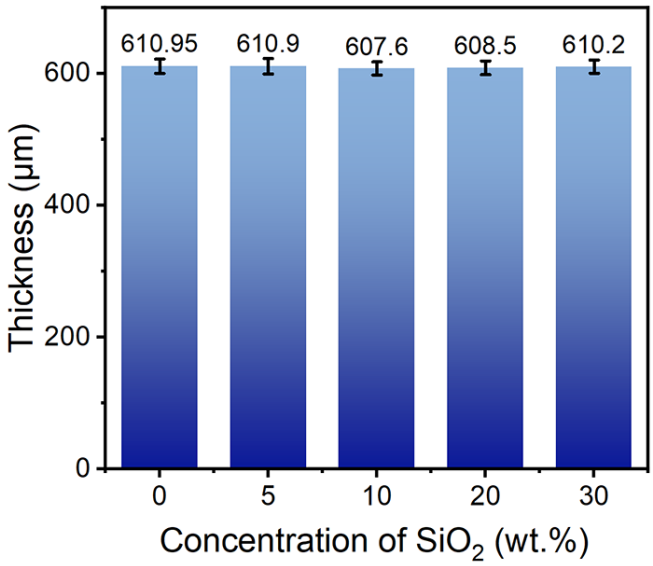

Figure S12. The thickness of highly aligned PAN-SiO_2 nanofiber/NW composite membranes with different concentrations of SiO_2 NPs.

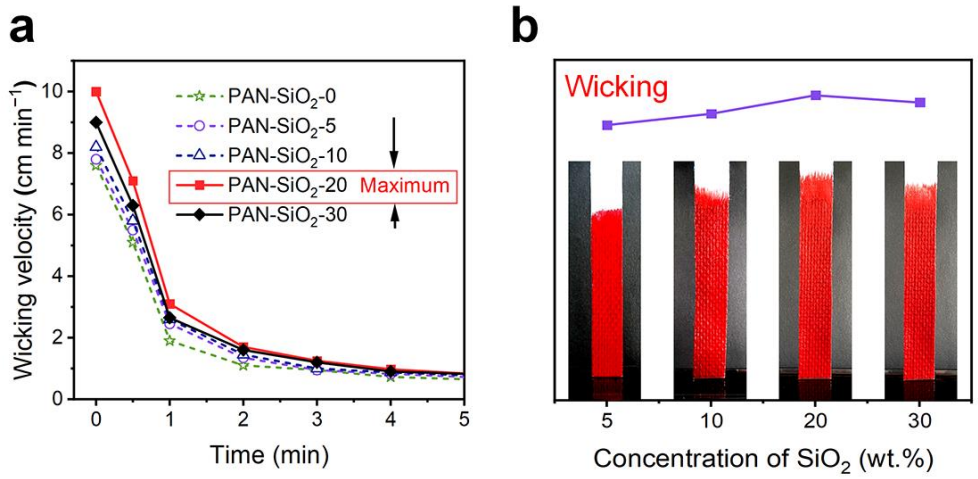

Figure S13. Wetting behavior of the PAN nanofiber/NW composite membranes with different concentrations of SiO_2 NPs: (a) wicking height and (b) Optical photographs.

Table S1. Humidification performance of the nonwoven fabric and micro-/nanofibrous composite membranes.

Sample	Wicking velocity (cm 30min^{-1})	Water absorption (%)	Pressure drop (Pa)	Water evaporation rate (mL h^{-1})	Humidity capacity (mL h^{-1})
Nonwoven	9.3	346	0	0.28	327
Composite membranes	19.5	497.7	14.4	0.34	514

Table S2. Properties of PAN-SiO_2 precursor solutions with various SiO_2 NPs concentrations.

PAN (wt %)	SiO_2 NPs concentration (wt %)	Viscosity (cps)	Surface Tension (mN m^{-1})	Conductivity (uS cm^{-1})
10	0	1060.97	35.47	298
10	5	1253.03	35.42	290
10	10	2606.80	34.76	284
10	20	3226.46	34.12	278
10	30	4256.43	33.24	275

Table S3. XPS data of PAN-SiO_2 NFMs with different concentrations of SiO_2 NPs.

SiO_2 NPs concentration (wt %)	**Atomic content (%)**			
	C	**N**	**O**	**Si**
0	75.75	19.78	4.47	0
5	74.80	20.63	4.07	0.50
10	73.28	20.21	5.33	1.18
20	69.48	19.75	8.10	2.67
30	63.22	17.78	13.46	5.54

Movie S1.

Water transport process from the top view of the random PAN NFM, the 200 μL red ink droplet was dropped on the surface of membrane.

Movie S2.

Water transport process from the top view of the highly aligned PAN NFM, the 200 μL red ink droplet was dropped on the surface of membrane.

Movie S3.

Wetting behavior of the highly aligned PAN-SiO_2-0 nanofiber/NW composite membrane, the 5 μL water was dropped on the surface of membrane.

Movie S4.

Wetting behavior of the highly aligned PAN-SiO_2-5 nanofiber/NW composite membrane, the 5 μL water was dropped on the surface of membrane.

Movie S5.

Wetting behavior of the highly aligned PAN-SiO_2-10 nanofiber/NW composite membrane, the 5 μL water was dropped on the surface of membrane.

Movie S6.

Wetting behavior of the highly aligned PAN-SiO_2-20 nanofiber/NW composite membrane, the 5 μL water was dropped on the surface of membrane.

Movie S7.

Wetting behavior of the highly aligned PAN-SiO_2-30 nanofiber/NW composite membrane, the 5 μL water was dropped on the surface of membrane.